

## Simulated Speed Distributions for Effusing Gases in the Transition Region

Phillip G. Wahlbeck<sup>‡</sup>

Department of Chemistry, Wichita State University, Wichita, Kansas 67260-0051

Received: April 20, 2005; In Final Form: August 1, 2005

Monte Carlo techniques were used to evaluate the flow of molecules through an ideal orifice (effusion) as predicted by isotropy-failure theory. Binary collisions of molecules were treated using classical mechanics with random numbers used for molecular speeds, directions, and recoil angles. Isotropy-failure theory was applied to give the dependence on pressure of the gas. Isotropy-failure theory assumes that the probability of escape is increased by the absence of the container wall where the orifice is located. The simulation was performed for Ar at 1000 K for  $10^7$  collisions. The simulation provided the number of molecules and their speeds in the orifice direction as a function of the isotropy-failure parameter  $d\omega/2\pi$  (related to the Knudsen number defined as the mean-free path divided by orifice diameter). As  $d\omega/2\pi$  increased (Knudsen number decreased, pressure increased) the transmission probability of the orifice increased, and the average speed of molecules escaping along the orifice normal increased. The results are compared to experimental results for the orifice transmission probability and speed distribution.

### Introduction

Effusion of gases from a container with an orifice into vacuum was studied initially by Knudsen.<sup>1–3</sup> Types of orifices that have been considered are the following: ideal, a hole located in a plane (no thickness); cylindrical, a circular hole located in a thick sheet; and other geometrical shapes, e.g., conical, hyperbolic, and spherical. The effusion method was used extensively at elevated temperatures to measure vapor pressures<sup>4</sup> of materials with low volatilities. References to earlier studies of effusion are given in Cater<sup>5</sup> and in Wahlbeck.<sup>4</sup>

The kinetic theory of gases provides a foundation for effusion; see Kennard.<sup>6</sup> For an ideal orifice, the angular number distribution should follow the cosine law, i.e.,

$$dN_\theta = N \bar{C} \cos \theta (d\Omega/4\pi) \quad (1)$$

where  $dN_\theta$  is the number of molecules (“molecules” is used for atomic cases also) effusing in unit time from a gas container with  $N$  molecules/unit volume with an average velocity of  $\bar{C}$  through an orifice of unit area through a solid angle of  $d\Omega$  subtended from the orifice at an angle of  $\theta$  from the normal to the orifice plane. Clausing<sup>7–9</sup> developed the formalism for the angular number distribution for nonideal orifices. The total number of molecules effusing can be determined by integrating the angular distributions.

Speed distributions for molecules in a gas container are given by the Maxwell–Boltzmann<sup>10</sup> distribution, i.e.,

$$dN_C/N = AC^2 \exp(-MC^2/2RT) dC \quad (2)$$

where  $dN_C/N$  is the fraction of molecules with speeds between  $C$  and  $C + dC$ ,  $M$  is the molar mass of the gas,  $R$  is the universal gas constant,  $T$  is the absolute temperature, and  $A$  is a constant. For effusing molecules, the speed distribution of eq 2 must have an additional multiplier of  $C$  [this is related to the  $\bar{C}$  of eq 1].

For atoms passing through a toothed-disk velocity selector possessing a constant resolution,  $\Delta C/C$ , the speed distribution of eq 2 must have an additional multiplier of  $C^2$ .

Velocity selectors are of two types. Miller and Kusch<sup>11</sup> used a rotating drum cut with helical slots. At a particular rotational velocity, only molecules within a narrow velocity range would pass. Hostettler and Berstein<sup>12</sup> developed a toothed-disk velocity selector that operated on the same principle as the drum with helical slots. These velocity selectors operate with a constant resolution,  $\Delta C/C$ . A second type of velocity selector is a time-of-flight selector. Molecules are pulsed over a short time to start trajectories, and the velocities of the molecules determine the time of arrival at a detector giving a flight-time distribution. Scott, Bauer, Wachman, and Trilling<sup>13</sup> used this type of velocity selector. The output data for these two selectors have an inverse relationship; the speed and flight time are inversely related.

The flow of molecules through an orifice is dependent on the pressure and temperature of the gas. The Knudsen number,  $Kn$ , is defined as  $\lambda/d$ , the mean-free path divided by the orifice diameter ( $\lambda$  and  $d \gg$  molecular dimensions). Approximately for  $Kn > 10$ , the flow is called molecular flow, and the kinetic theory of gases is valid. For  $Kn < 0.01$ , the flow is fluid or hydrodynamic flow. For  $0.01 < Kn < 10$ , the flow is known as the transition region between molecular flow and hydrodynamic flow.

Wahlbeck<sup>14</sup> developed the isotropy-failure theory to account for flow dependence on  $Kn$ . The principle is that the flow is influenced by the presence of the orifice opening into a vacuum. The absence of molecules moving through the orifice (from the vacuum) toward collision sites inside the gas container increases the probability for molecules effusing. The major assumptions are (1) the probability of escape from the orifice was assumed to be linearly dependent on the solid angle subtended by the orifice at the collision site, (2) for a given  $Kn$ , a distribution of free paths was used to give the mean-free path, and (3) the angular dependence (measured from the normal to the orifice plane) of the solid angle subtended by the orifice at the collision site relative to the orifice plane was assumed to be given by

<sup>‡</sup> Phone: 316-978-7083. Fax: 316-978-3431. E-mail: Phillip.Wahlbeck@wichita.edu.

the cosine function. A parameter,  $d\omega/2\pi$  (originally labeled as  $d\bar{\omega}/2\pi$ ), was derived, which is related to the solid angle subtended by the orifice and describes all three regions of flow;  $d\omega/2\pi$  was given by

$$d\omega/2\pi = 1 - (\pi r/2\lambda)[H_1(r/\lambda) - Y_1(r/\lambda)] + r/\lambda \quad (3)$$

where  $H_1(x)$  is a Struve function and  $Y_1(x)$  is a Bessel function of the second kind. A table of orifice transmission probabilities for circular orifices of varying lengths and varying Kn values may be found in Wahlbeck.<sup>4</sup>

Experimental data on the number of molecules flowing through orifices fall into two categories: total number of molecules and angular number distributions. The studies for angular number distributions were reported by Stickney et al.<sup>15</sup> and by Wang and Wahlbeck.<sup>16</sup> The total number of molecules effusing was studied by Carlson et al.<sup>17</sup> and by Liepmann;<sup>18</sup> these studies were in agreement with the results of the isotropy-failure theory.<sup>14</sup> For a near-ideal orifice, the probability of molecules effusing along the orifice normal increased in accordance with isotropy-failure theory.

Experimental speed distributions for effusion through thin-edged orifices were reported by Miller and Kusch,<sup>11</sup> Scott et al.,<sup>19</sup> and Wang and Wahlbeck<sup>20</sup> using a drum or toothed-disk velocity selector. Lou and Stickney<sup>21</sup> and Scott et al.<sup>13</sup> used time-of-flight measurements. Estermann, Simpson, and Stern<sup>22</sup> used gravity in order to velocity select molecules (related to flight-time studies). At large Kn, the experimental results showed agreement with the Maxwell–Boltzmann<sup>10</sup> distribution. Lou and Stickney<sup>21</sup> observed excellent agreement with the Maxwell–Boltzmann distribution at Kn = 18 independent of the angle of effusion,  $\theta$ . Experimental results<sup>19,21</sup> for a near-ideal orifice showed that the average speed increased as Kn decreased. With the time-of-flight experiments,<sup>13</sup> a decrease in the number of slow molecules was indicated. With the velocity selectors, an increase in high-speed molecules was observed in addition to a decrease in slow molecules.

Early Monte Carlo simulations for effusion were performed by Ward, Mulford, and Kahn.<sup>23</sup> These simulations showed that at very large Kn the effusion cell functions like a pinhole camera.

The purpose of the present study was to find the influence of isotropy-failure theory on velocity distributions of effusing molecules. The analytical results of isotropy-failure theory<sup>14</sup> were in agreement with experimental data for the number of molecules effusing. Monte Carlo simulations provided a second approach to isotropy-failure theory, and it provided velocity distribution predictions as well as numbers of molecules effusing. The physics of binary collision processes was used. The simulation results are for a large number of molecules undergoing binary collisions. The number of molecules effusing and the speed distribution for the normal to the plane of an ideal orifice will be compared with the simulated number distributions and the simulated speed distributions of molecules effusing along the normal to the plane of the ideal orifice.

### Simulation Calculations

**Model and Overview of Calculations.** Monte Carlo simulation calculations were performed for Ar at 1000 K. Calculations were performed for binary gas-phase collisions occurring in a gas contained in a vessel with an ideal orifice, i.e., a circular opening in a plane. Escaping molecules leave their last collision site at a distance  $\lambda$  from the orifice plane. Classical mechanics was used for the elastic collision process for an individual hard-

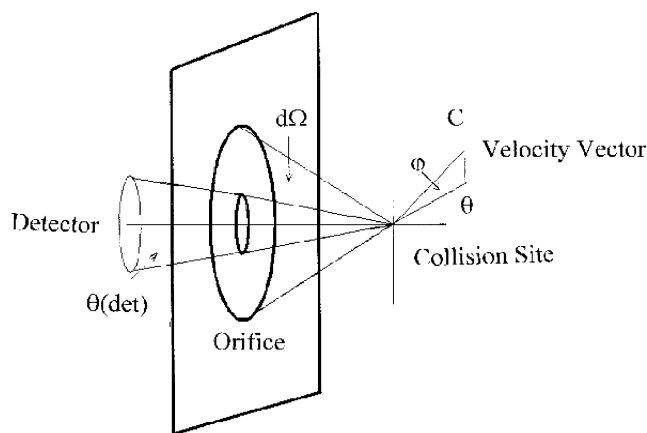


**Figure 1.** A representation of the orifice and the collision site with coordinates for an arriving molecule given as  $C$ ,  $\theta$ ,  $\varphi$ . The solid angle subtended at the collision site by the orifice is  $d\Omega$ . The detector acceptance geometry was determined by  $\theta(\text{det})$ .

sphere collision of two molecules with size. Assumption 1 of the original theory was retained, i.e., the probability of escape is linearly dependent on the solid angle subtended by the orifice area (open to a vacuum) toward the collision site. Two simplifying assumptions were made: (1) only a fixed free path was chosen equal to the mean-free path and (2) the collision site was located along the normal to the orifice plane. The calculations were for an ensemble of  $10^7$  collisions in increments of 250 000 with a given distance between the collision site and the orifice, and these calculations were repeated for varying distances of the collision site from the orifice,  $\lambda$ , related to the Knudsen number Kn.

**Mathcad and Random Number Generation.** The calculations were performed with Mathcad.<sup>24</sup> Mathcad has a random number generator, and the determination of  $5 \times 10^6$  random numbers showed no repeatability. With Mathcad it is necessary to input a “seed value” into the random number generator. Values for this “seed value” were selected with the random number generator on a Sharp Scientific calculator, EL-509RH.

**Collision Process, Parameters for Colliding Molecules.** A molecular collision involves two molecules colliding at a position in the gas container. A molecule has a speed established by a random number, and a direction established by random numbers for two spatial coordinates. The vector for each molecule in three-dimensional laboratory coordinates was given by  $C$ ,  $\theta$ ,  $\varphi$ .

The principle of isotropy-failure theory<sup>14</sup> is that molecules cannot arrive at the collision site if their origin is outside the ideal orifice. Consequently values of  $\theta$  were limited in accord with the solid angle subtended by the orifice,  $d\Omega$ . The choice of coordinates is shown in Figure 1.

The random values for  $C$  of the two molecules were constrained so that a Maxwell–Boltzmann speed distribution<sup>10</sup> was attained. The physics of the collision process for the two atoms was taken from Jeans.<sup>25</sup> One converts the laboratory velocity vectors for the two colliding molecules into relative coordinates to generate a center-of-mass vector and two equal but opposing relative vectors. After the collision, the molecules move with relative coordinates changed in direction and with the center-of-mass vector continuing unchanged.

**Impact Parameter for Molecules with Size.** The size of a molecule influences the outcome of the calculations through the impact parameter.<sup>26</sup> As the two molecules (relative motion vectors) are opposed to each other, the molecules do not collide

precisely on the same line. The off-centeredness of the two molecules gives rise to a recoil angle effect as discussed by Jeans.<sup>25</sup> The cross-section for the collision may be calculated from the overlap of the two molecular cross sections,

$$R = 2r^2 \arccos(s/r) - 2s(r^2 - s^2)^{0.5} \quad (4)$$

where  $r$  is the radius of the molecule and  $s$  is the distance between two lines, each parallel to the relative velocity vectors and passing through the centers of the two molecules. The distance  $s$  is the "impact parameter" of chemical kinetics<sup>26</sup> used to describe collisions between molecules. The recoil angle was selected by the random number generator for values of  $\theta(\text{rec})$ ,  $\varphi(\text{rec})$  with the constraint that they must fit the distribution given by eq 4. The directions of the relative vectors for the two colliding molecules were modified by adding  $\theta(\text{rec})$  and  $\varphi(\text{rec})$ . It was possible then to calculate the vectors for the molecules after the collision in laboratory coordinates.

**Speeds of Molecules Leaving the Orifice in the Forward Direction.** Simulated results for the flow of gases from orifices are for molecules leaving the orifice toward a detector, i.e., molecules having  $\theta < \theta(\text{det})$  in Figure 1. Molecules with velocity vectors of  $-5^\circ < \theta < 5^\circ$ , the values chosen for  $\theta(\text{det})$ , were examined for the number of molecules and for their speed distributions.

The speed distributions could be evaluated for (1) the distribution after collision, (2) the distribution for effusing molecules, and (3) the distribution as observed with a toothed-disk velocity selector.

**Simulated Speed Distributions.** Experimental results gave speed distributions for molecules effusing. These have been characterized by giving  $C(\text{average})$ ,  $C(\text{most probable})$ ,  $C(\text{lower } C \text{ at } I = 1/2 I(\text{max}))$ , and  $C(\text{upper } C \text{ at } I = 1/2 I(\text{max}))$ . To obtain such values from the simulation program, it was necessary to use a limited number of collisions, 150 000. The "seed value" used for the random number generator was chosen to give an average  $C$  close to the average calculated for  $10^7$  collisions.

## Simulation Results

**Simulated Velocities and the Collision Process.** The velocities of molecules arriving at the collision site and the velocities of molecules leaving the collision site were calculated with the simulation program. The results for  $\text{Kn} = 1$  for 2000 collisions are shown in Figure 2. The presence of the orifice does not allow molecules to arrive at the collision site through the solid angle  $d\Omega'$ . As seen from Figure 2, an increase in velocities through the orifice to the detector is shown for molecules leaving collision sites.

**Number of Molecules Effusing.** Simulations were performed for Knudsen numbers,  $\text{Kn}$ , from 100 to 0.01. The number of molecules leaving the ideal orifice toward the detector for  $-5^\circ < \theta(\text{det}) < 5^\circ$  was calculated. These results are given in Table 1.

**Speed Distributions of Effusing Molecules.** From the values of the speeds,  $C$ , of molecules leaving the orifice in the angular zone  $\theta(\text{det})$ , average speeds were calculated for the  $10^7$  collisions in the gas container. The average speeds that were calculated from the simulation are the following:  $C(\text{average})$ ,  $C$  average after collisions;  $C(\text{after})$ ,  $C$  average after effusion, and  $C(\text{vel sel})$ ,  $C$  average as determined by a toothed-disk velocity selector. These average speeds may be compared with the expected Maxwell-Boltzmann speed distributions<sup>10</sup> for the same conditions:  $C(\text{average})$ ,  $C(\text{after})$ , and  $C(\text{vel sel})$ . The results are given in Table 2.

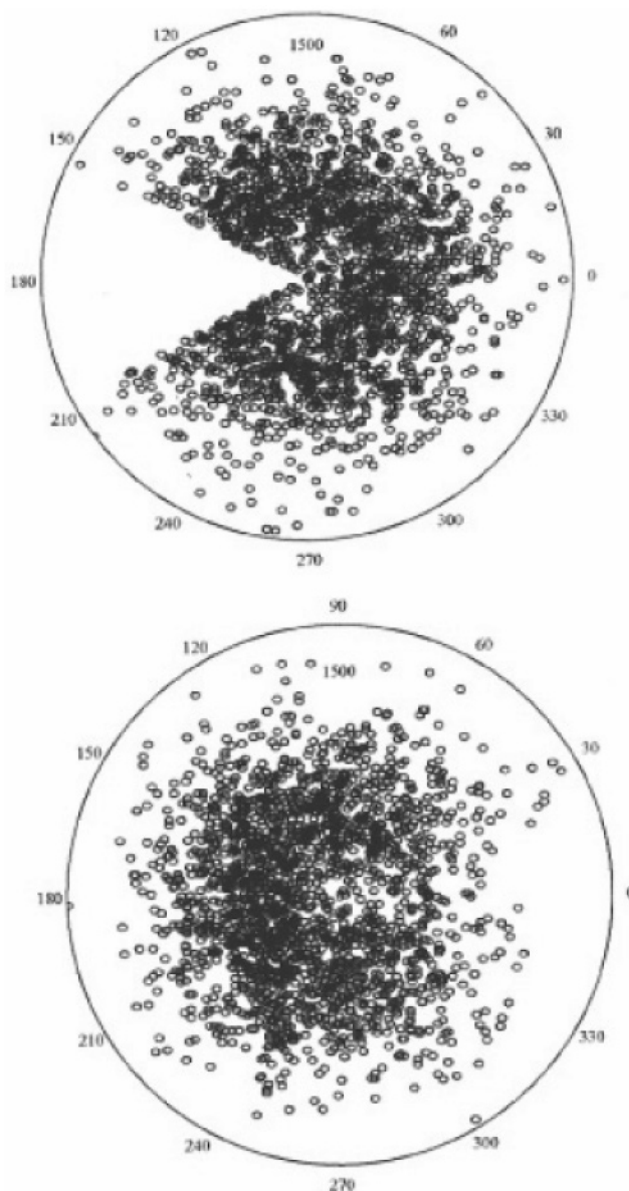


**Figure 2.** Simulation results for the case of  $\text{Kn} = 1$  and 2000 collisions. The upper data are for molecules arriving at the collision site; speeds are plotted vs  $\theta$  (the data are symmetrical for  $\varphi$ ). Isotropy failure (the orifice position) limited the  $\theta$  values. The lower data are for molecules after collision, speed plotted versus  $\theta$ . From the speeds it can be seen that there is an increase in the speed distribution toward the orifice.

Limited calculations were performed for establishing the relationships among (1) the average speed, (2) the most probable speed, (3) the lower speed at  $I = 1/2 I(\text{max})$ , and (4) the upper speed at  $I = 1/2 I(\text{max})$ . For these simulations, 150 000 collisions were used. These results are shown in Figure 3.

## Discussion

Isotropy-failure theory was developed and applied to the effusion process earlier.<sup>14</sup> The early applications were to the number of molecules effusing as a function of  $\text{Kn}$ . The present Monte Carlo simulations using isotropy-failure theory with the simplifying assumptions have been applied to the number of molecules effusing but in addition examine the predicted effect on the velocity distributions.

**Number of Molecules Effusing.** In the model being considered, the simulation is for an ensemble of binary collisions. The gas in the container is considered to be uniform with no



**TABLE 1: Calculated Numbers of Molecules from an Ideal Orifice**

Knudsen no. (Kn)	$d\omega/2\pi^a$	$N(\text{effusing})^b$	$N/N(\text{Kn}=100)$
100	0.000493	2492.3	1
50	0.009739	2497.4	1.00205
25	0.019092	2491.7	0.99977
10	0.045446	2523.1	1.01234
5	0.085097	2579.5	1.03500
2	0.189140	2727.0	1.09418
1	0.303331	2992.1	1.20055
0.7	0.380880	3197.1	1.28279
0.4	0.516425	3657.1	1.46734
0.3	0.587790	3914.0	1.57045
0.2	0.683421	4258.3	1.70856
0.1	0.816770	4725.4	1.89600
0.05	0.902650	4996.8	2.00490
0.02	0.960181	5180.1	2.07842
0.01	0.9815	5241.4	2.10302

<sup>a</sup> Values of  $d\omega/2\pi$ , the isotropy-failure parameter, were calculated from eq 3. <sup>b</sup> The values of  $N$  are the average numbers of molecules leaving the orifice in the angular zone of  $\theta(\text{det}) < 5^\circ$  per 250 000 collisions occurring inside the vacuum container. The total number of collisions considered was  $10^7$ .

**TABLE 2: Simulated Speed Results**

Knudsen no. (Kn)	$d\omega/2\pi$	$C(\text{after})/C(\text{bar})^a$	$C^3/C(\text{beam})^a$	$C^4/C(\text{vel sel})^a$
100	0.000493	1.00875	1.00602	1.00476
50	0.009739	1.00922	1.00661	1.00518
25	0.019092	1.00845	1.00654	1.00565
10	0.045446	1.00874	1.00624	1.00506
5	0.085097	1.00935	1.00674	1.00550
2	0.189140	1.01218	1.00885	1.00681
1	0.303331	1.01679	1.01251	1.01022
0.7	0.380880	1.02058	1.01411	1.01051
0.4	0.516425	1.02727	1.01954	1.01488
0.3	0.587790	1.03126	1.02195	1.01699
0.2	0.683421	1.03527	1.02475	1.01867
0.1	0.816770	1.03934	1.02775	1.02090
0.05	0.902650	1.04267	1.03054	1.02372
0.02	0.960181	1.04273	1.03035	1.02321
0.01	0.9815	1.04348	1.03054	1.023056

<sup>a</sup> Values for Ar at 1000 K are  $C(\text{bar}) = 727.207$  m/s,  $C(\text{beam}) = 856.235$  m/s,  $C(\text{vel sel}) = 968.074$  m/s.

pressure gradient. The results of the simulation of effusion from an ideal orifice are given in Table 1 and shown graphically in Figure 4. The number of molecules leaving the orifice divided by the number leaving the orifice at  $\text{Kn} = 100$ ,  $N/N(\text{Kn}=100)$ , is plotted vs  $d\omega/2\pi$ , the isotropy-failure parameter [see eq 3]. The value of  $N$  at  $\text{Kn} = 100$  should represent molecular flow conditions based on the kinetic theory of gases, eq 1. The value of  $N/N(\text{Kn}=100)$  is the orifice transmission probability to the detector for  $-5^\circ < \theta(\text{det}) < 5^\circ$  relative to effusion conditions for  $\text{Kn} = 100$  through the same angular zone. For  $d\omega/2\pi$  of 0 molecular flow should occur, and for  $d\omega/2\pi = 1$  hydrodynamic flow should occur. From Table 1 the values of  $d\omega/2\pi$  for  $\text{Kn} = 100$  and 0.01 are respectively 0.000493 and 0.9815. The transition region is described in Figure 4 by intermediate values of  $d\omega/2\pi$ .

The results of the simulation may be compared with results from an analytical integration of isotropy-failure<sup>14</sup> equations. The simulation for effusion through the detector solid angle gave a more detailed functional form for the orifice transmission probability, which showed a curved dependence of the orifice transmission probabilities on  $d\omega/2\pi$ .

The orifice transmission probability from the simulation may be compared with experimental values from Wang and Wahl-

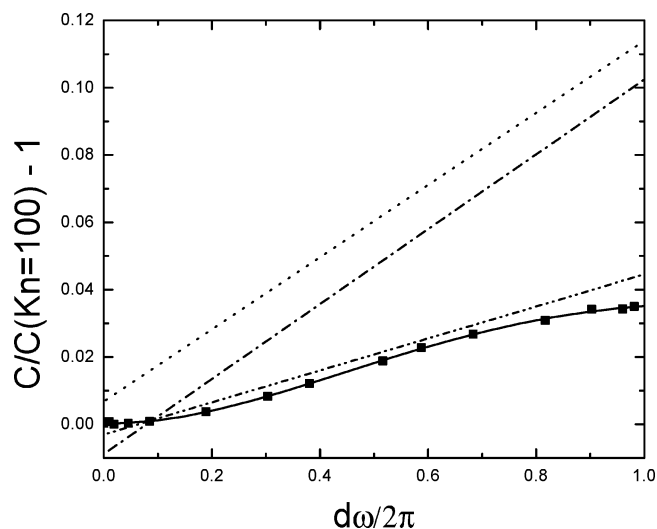


**Figure 3.** Simulated speed distribution results referenced to results for  $\text{Kn} = 100$  vs  $d\omega/2\pi$ , the isotropy-failure parameter. The simulated  $C$  (average), square points and solid line, values are for  $10^7$  collisions. The dashed lines from top to bottom are  $C(\text{lower})$  at  $I = 1/2 I(\text{max})$ ,  $C(\text{most probable})$ , and  $C(\text{upper})$  at  $I = 1/2 I(\text{max})$ ; these are for a limited simulation of 150 000 collisions. Dashed lines are least-squares lines.

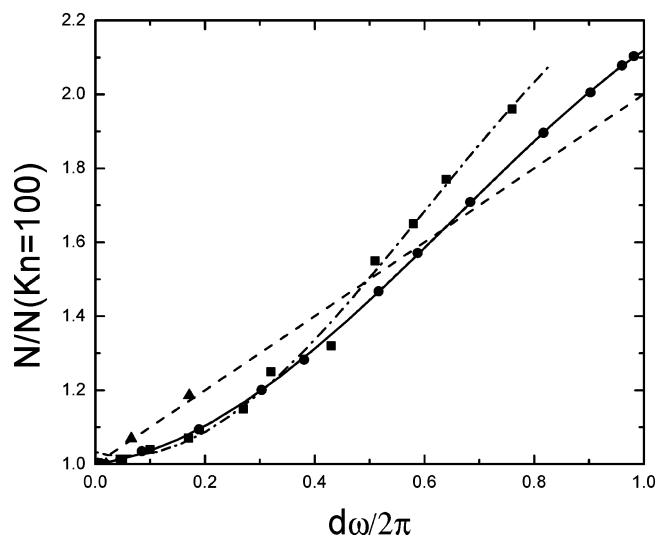


**Figure 4.** Data for the number of molecules effusing (circles and solid line) referenced to the number at  $\text{Kn} = 100$  (orifice transmission probability) vs  $d\omega/2\pi$ , the isotropy-failure parameter. Experimental data are from Wang and Wahlbeck<sup>16</sup> (squares) and Stickney et al.<sup>15</sup> (triangles).

beck<sup>16</sup> and from Stickney et al.<sup>15</sup> in Figure 4. The agreement of the experimental data of Wang and Wahlbeck<sup>14</sup> with the simulation results is excellent for  $d\omega/2\pi$  less than 0.5, and the orifice transmission probability is larger than predicted for larger  $d\omega/2\pi$ . The experimental data of Stickney et al.<sup>15</sup> are more limited and in agreement with the linear theoretical result.

**Speed Distribution Results.** As indicated in the Introduction, average speeds for molecules through the detector solid angle may be simulated (1) for the molecules immediately after collision, (2) for the molecules which have effused (a  $C^3$  distribution), and (3) for molecules which passed through a velocity selector (a  $C^4$  distribution). These average speeds are shown in Figure 5 from the simulation as a function of  $\text{Kn}$ . The largest effect is for the speed after collision followed in order by the effusion speed and the velocity selector speed.

Experimental speed distributions have been reported in different ways: average speed, most probable speed, lower speed

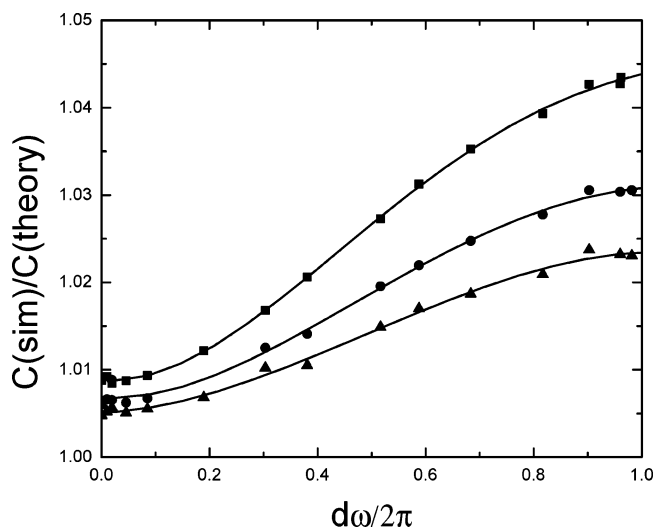


**Figure 5.** Simulated results for the ratio of  $C/C(\text{theory})$  vs  $d\omega/2\pi$ , the isotropy-failure parameter, for the average speeds after collisions occur (squares), for molecules effusing ( $C^3$ , circles), and for molecules passing through a velocity selector ( $C^4$ , triangles).  $C(\text{theory})$  is the average speed using the Maxwell–Boltzmann speed distribution.

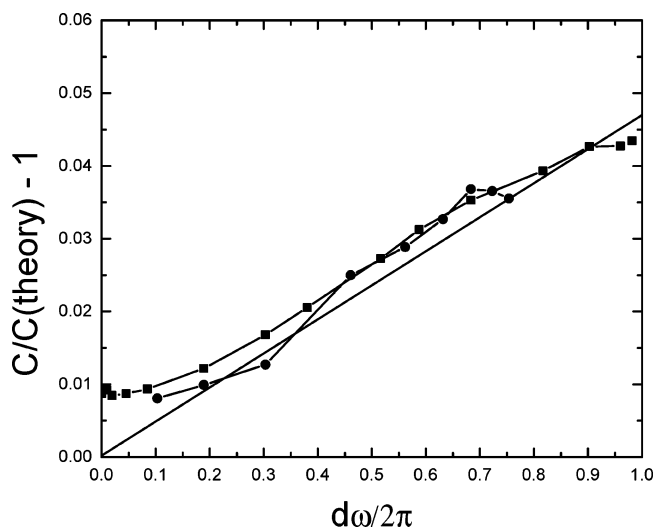


**Figure 6.** Comparison of  $(C/C(\text{theory}) - 1)$  vs  $d\omega/2\pi$ , the isotropy-failure parameter, for the simulated results for  $C(\text{average})$  after collisions (squares), for the simulated results (straight line) for  $C(\text{upper})$  at  $I = 1/2 I(\text{max})$ , and for the experimental results (circles) of Scott et al.<sup>19</sup> for  $C(\text{upper})$  at  $I = 1/2 I(\text{max})$ .

at  $I = 1/2 I(\text{max})$ , and upper speed at  $I = 1/2 I(\text{max})$ . Simulation results for these different types of speeds as a function of  $d\omega/2\pi$  are shown in Figure 3. The simulation results (with a limited number of collisions) for the average  $C$  are shown to agree best with the values of  $C(\text{upper})$  at  $I = 1/2 I(\text{max})$ .

Experimental results from velocity selectors by Scott et al.<sup>19</sup> and by Wang and Wahlbeck<sup>20</sup> for molecules leaving near-ideal orifices in the forward direction agreed with the Maxwell–Boltzmann<sup>10</sup> speed distribution. Results for the transition region showed that there was an excess of molecules with higher velocities (or a decrease in the number of molecules with lower speeds). The data of Scott et al.<sup>19</sup> for a near-ideal orifice,  $L/d = 0.1$ , were analyzed to provide results for the speeds after the collisions inside the gas container. Their data for  $C(\text{upper})$  for  $I = 1/2 I(\text{max})$  provided results with small uncertainties over a large range of Kn values as shown in Figure 6. For comparison the simulation data for an ideal orifice for the average speed and for the limited simulation for the  $C(\text{upper})$  for  $I = 1/2 I(\text{max})$

are shown. The agreement among these data is excellent. The data of Wang and Wahlbeck<sup>20</sup> for molecules which passed through a near-ideal orifice,  $L/d = 0.026$ , through a velocity selector had a large uncertainty, which did not permit one to see a dependence of Kn. The theoretically expected change according to the isotropy-failure theory is less than 0.02 in the average velocity; the experimental scatter in the data was approximately 0.03.

Data from time-of-flight experiments<sup>13</sup> have been too limited to draw detailed conclusions. Plots of the data of Scott et al.<sup>13</sup> show that the most probable speed increased as Kn decreased.

The data of Wang and Wahlbeck<sup>20</sup> for cylindrical orifices indicated that there was a dependence on the speeds of molecules (after passing through the velocity selector) on Kn. This dependence on Kn was stronger for cylindrical orifices than for near-ideal orifices. At this time, simulations for cylindrical orifices have not been performed.

## Conclusions

Monte Carlo methodology yielded results for the flow of molecules through an orifice into vacuum. The theoretical bases of the calculations were classical mechanics for the collision process and the isotropy-failure theory.<sup>14</sup> When using the Knudsen method to measure vapor pressures,<sup>4</sup> care should be taken either to use only molecular flow data ( $\text{Kn} > 10$ ) or to make corrections to data with the  $d\omega/2\pi$ , the isotropy-failure parameter.

The simulated results for the number of molecules flowing through the orifice as dependent on  $d\omega/2\pi$  (related to the value of the Knudsen number, Kn) were in good agreement with the experimental results of Wang and Wahlbeck<sup>16</sup> and in qualitative agreement with the results of Stickney et al.<sup>15</sup>

The simulated results for the speed distributions for an ideal orifice are in agreement with (1) the Maxwell–Boltzmann<sup>10</sup> distribution for molecular flow conditions when Kn is large., (2) general trends in the dependence on Kn observed by Scott et al.<sup>13</sup> and by Lou and Stickney,<sup>21</sup> and (3) quantitative results from Scott et al.<sup>19</sup>

**Acknowledgment.** The support of Wichita State University and the Department of Chemistry was appreciated. Colleagues in the high-temperature community are thanked for their input in discussions of this work. Professor W. R. Carper is thanked for his helpful ideas and encouragement.

## References and Notes

- (1) Knudsen, M. *Ann. Phys. (Weinheim, Ger.)* **1909**, 28, 75.
- (2) Knudsen, M. *Ann. Phys. (Weinheim, Ger.)* **1909**, 28, 999.
- (3) Knudsen, M. *Ann. Phys. (Weinheim, Ger.)* **1909**, 29, 179.
- (4) Wahlbeck, P. G. *High Temp. Sci.* **1986**, 21, 189.
- (5) Cater, E. D. *Proceedings of the 10<sup>th</sup> Materials Research Symposium on Characterization of High-Temperature Vapors and Gases*; U.S. NBS Special Publication No. 561, September 1978, issued 1979; p 3.
- (6) Kennard, E. H. *Kinetic Theory of Gases*; McGraw-Hill Book Co.: New York, 1938; p 60 ff.
- (7) Clausing, P. *Physica* **1929**, 9, 65.
- (8) Clausing, P. *Z. Physik* **1930**, 66, 471.
- (9) Clausing, P. *Ann. Phys. (Weinheim, Ger.)* **1932**, 12, 961.
- (10) See physical chemistry texts; e.g., Atkins, P. *Physical Chemistry*, 6th ed.; Freeman: New York, 1998; p 25.
- (11) Miller, R. C.; Kusch, P. *Phys. Rev.* **1955**, 99, 1314.
- (12) Hostettler, H. U.; Berstein, R. B. *Rev. Sci. Instrum.* **1960**, 31, 872.
- (13) Scott, P. B.; Bauer, P. H.; Wachman, H. Y.; Trilling, L. *Rarefied Gas Dyn., Symp.* **1967**, 2, 1353.
- (14) Wahlbeck, P. G. *J. Chem. Phys.* **1971**, 55, 1709.
- (15) Stickney, R. E.; Keating, R. F.; Yamamoto, S.; Hastings, W. J. *J. Vac. Sci. Technol.* **1967**, 4, 10.
- (16) Wang, K. C.; Wahlbeck, P. G. *J. Chem. Phys.* **1967**, 47, 4799.

- (17) Carlson, K. D.; Gilles, P. W.; Thorn, R. J. *J. Chem. Phys.* **1963**, *38*, 2725.  
 (18) Liepmann, H. W. *J. Fluid Mech.* **1961**, *10*, 65.  
 (19) Scott, J. E., Jr.; Morton, H. S., Jr.; Phipps, J. A.; Moonan, J. F.; *Rarefied Gas Dyn., Symp. 4* **1966**, *2*, 331.  
 (20) Wang, K. C.; Wahlbeck, P. G. *J. Chem. Phys.* **1970**, *53*, 2896.  
 (21) Lou, Y. S.; Stickney, R. E. *Phys. Fluids* **1970**, *13*, 528.  
 (22) Estermann, I.; Simpson, O. C.; Stern, O. *Phys. Rev.* **1947**, *71*, 238.

- (23) Ward, J. W.; Mulford, R. N. R.; Kahn, M. *J. Chem. Phys.* **1967**, *47*, 1710. Ward, J. W.; Mulford, R. N. R.; Bivins, R. L. *J. Chem. Phys.* **1967**, *47*, 1718. Ward, J. W. *J. Chem. Phys.* **1967**, *47*, 4030.  
 (24) *Mathcad Plus*, version 6.0 professional; MathSoft Inc.: Cambridge MA.  
 (25) Jeans, J. *The Dynamical Theory of Gases*, 4th ed.; University Press: Cambridge, UK, 1925; p 260.  
 (26) Moore, J. W.; Pearson, R. G. *Kinetics and Mechanism*, 3rd ed.; Wiley: New York, 1981; p 91.